

Influence of Cr doping on the stability and structure of small cobalt oxide clusters

Nguyen Thanh Tung, Nguyen Minh Tam, Minh Tho Nguyen, Peter Lievens, and Ewald Janssens

Citation: *The Journal of Chemical Physics* **141**, 044311 (2014); doi: 10.1063/1.4890500

View online: <http://dx.doi.org/10.1063/1.4890500>

View Table of Contents: <http://scitation.aip.org/content/aip/journal/jcp/141/4?ver=pdfcov>

Published by the [AIP Publishing](#)

Articles you may be interested in

[Half-metallicity and magnetism of GeTe doped with transition metals V, Cr, and Mn: A theoretical study from the viewpoint of application in spintronics](#)

J. Appl. Phys. **112**, 053902 (2012); 10.1063/1.4750031

[Copper doping of small gold cluster cations: Influence on geometric and electronic structure](#)

J. Chem. Phys. **135**, 224305 (2011); 10.1063/1.3664307

[Nature of Ar bonding to small Co \$n\$ + clusters and its effect on the structure determination by far-infrared absorption spectroscopy](#)

J. Chem. Phys. **130**, 034306 (2009); 10.1063/1.3058637

[Electronic structure and transport properties of doped CoSi single crystal](#)

J. Appl. Phys. **101**, 033715 (2007); 10.1063/1.2464186

[Atomic clusters of magnetic oxides: Structure and phonons](#)

J. Appl. Phys. **93**, 7379 (2003); 10.1063/1.1558252



AIP | Journal of
Applied Physics

Journal of Applied Physics is pleased to
announce **André Anders** as its new Editor-in-Chief

Influence of Cr doping on the stability and structure of small cobalt oxide clusters

Nguyen Thanh Tung,^{1,a)} Nguyen Minh Tam,² Minh Tho Nguyen,² Peter Lievens,¹ and Ewald Janssens^{1,b)}

¹Laboratory of Solid-State Physics and Magnetism, KU Leuven, B-3001 Leuven, Belgium

²Department of Chemistry, KU Leuven, B-3001 Leuven, Belgium

(Received 11 March 2014; accepted 7 July 2014; published online 29 July 2014)

The stability of mass-selected pure cobalt oxide and chromium doped cobalt oxide cluster cations, Co_nO_m^+ and $\text{Co}_{n-1}\text{CrO}_m^+$ ($n = 2, 3$; $m = 2-6$ and $n = 4$; $m = 3-8$), has been investigated using photodissociation mass spectrometry. Oxygen-rich Co_nO_m^+ clusters ($m \geq n + 1$ for $n = 2, 4$ and $m \geq n + 2$ for $n = 3$) prefer to photodissociate via the loss of an oxygen molecule, whereas oxygen poorer clusters favor the evaporation of oxygen atoms. Substituting a single Co atom by a single Cr atom alters the dissociation behavior. All investigated $\text{Co}_{n-1}\text{CrO}_m^+$ clusters, except CoCrO_2^+ and CoCrO_3^+ , prefer to decay by eliminating a neutral oxygen molecule. Co_2O_2^+ , Co_4O_3^+ , Co_4O_4^+ , and CoCrO_2^+ are found to be relatively difficult to dissociate and appear as fragmentation product of several larger clusters, suggesting that they are particularly stable. The geometric structures of pure and Cr doped cobalt oxide species are studied using density functional theory calculations. Dissociation energies for different evaporation channels are calculated and compared with the experimental observations. The influence of the dopant atom on the structure and the stability of the clusters is discussed.

© 2014 AIP Publishing LLC. [<http://dx.doi.org/10.1063/1.4890500>]

I. INTRODUCTION

Transition metal oxides have attracted long-standing interest in physics, chemistry, and material science due to their huge potential for applications in catalysis, electronics, and magnetic materials.¹⁻⁵ During the last two decades, their corresponding gas phase clusters have been investigated extensively, showing a non-monotonic dependence of properties on the number of constituent atoms and the cluster composition, which results in intriguing chemical and physical properties.⁶⁻⁹

In this regard, binary and doped transition metal oxide clusters have been designed artificially to understand the interplay between, on one hand, composition, cluster size, structure, shape and, on the other hand, their physical and chemical properties. For example, the evolution of electronic structures as a function of composition and charge state of $\text{MM}'\text{O}_7^{2-}$ and $\text{M}_2\text{O}_7^{2-}$ ($M, M' = \text{Cr}, \text{Mo}, \text{W}$) clusters was studied using photoelectron spectroscopy.¹⁰ Singly Ti for V substituted $(\text{V}_2\text{O}_5)_{n-1}(\text{VTiO}_5)^-$ ($n = 2-4$) cluster anions were shown to have polyhedral caged structures similar to those of their isoelectronic counterparts, the neutral $(\text{V}_2\text{O}_5)_n$ clusters.¹¹ The electronic and geometric structures of MoWO_y^- and MoVO_y^- were compared to their monometallic analogs, Mo_2O_y^- , W_2O_y^- , and V_2O_y^- ($y = 2-5$), using vibrationally resolved anion photoelectron spectroscopy.^{12,13} The electron transfer and the structures of $[(\text{CeO}_2)(\text{VO}_2)_{1,2}]^+$ and $[(\text{Ce}_2\text{O}_3)(\text{VO}_2)]^+$ clusters were discussed on the basis of in-

frared vibrational predissociation spectroscopy experiments and quantum chemical computations.¹⁴

Cobalt oxide species have been considered as one of the most fascinating systems, e.g., due to their capability to act as an efficient catalyst for water splitting and CO oxidation.¹⁵⁻¹⁸ Cobalt oxide nanoparticles can also be used in magnetic storage devices and sensor applications.¹⁹⁻²¹ Their stability, structures, chemical reactivities, ionization energies, dissociation energies, and magnetic properties are engaging and challenging subjects.²²⁻²⁷ Triggered by the above listed examples that illustrate the effect of dopant atoms on the properties of metal oxide clusters, we set out to investigate the influence of chromium dopants on the structure and stability of cobalt oxide clusters. These clusters likely have interesting magnetic properties, since Co and Cr, both 3d transition metals, are ferromagnetic and antiferromagnetic in bulk, respectively. Moreover, cobalt-chromium oxide systems attract attention due to their potential to produce large magnetoelectric effects, in particular in the multiferroic spinel CoCr_2O_4 , which demonstrates simultaneously ferroelectricity and ferromagnetism.^{5,28,29} More insight into the size- and constituent-dependent structure and stability of cobalt-chromium oxide clusters may eventually allow to control and tune the functionality of multiferroics at the atomic scale.

The stability of a cluster is reflected in many size-dependent properties, such as abundances, ionization energies, and dissociation energies. If excess energy is provided by external manipulations, e.g., by photoexcitation, the cluster stability can be investigated via induced fragmentation.³⁰⁻³⁸ Statistical models in combination with photofragmentation spectroscopy can be used to extract the relative dissociation energies that are associated with cleavages of different bonds.

^{a)}Present address: Institute of Materials Science, Vietnam Academy of Science and Technology, Vietnam.

^{b)}ewald.janssens@fys.kuleuven.be

This approach has been followed to study the stability of size-selected clusters, showing that the dissociation channels are governed by relative stabilities of the daughter clusters.^{30–32} In addition, more stable clusters, characterized by larger dissociation energies, are known to remain more abundant after fragmentation and they are produced as preferred fragments from larger clusters.^{34–38}

In this work, the size- and dopant-dependent fragmentation behavior of Co_nO_m^+ and $\text{Co}_{n-1}\text{CrO}_m^+$ ($n = 2, 3; m = 2–6$ and $n = 4; m = 3–8$) clusters is investigated by means of laser dissociation and mass spectrometry. Density functional theory (DFT) calculations are performed for selected species to further explore the structures and dissociation energies of the clusters.

II. EXPERIMENTAL AND THEORETICAL METHODS

The pure cobalt and chromium doped cobalt oxide cluster cations, Co_nO_m^+ and $\text{Co}_{n-1}\text{CrO}_m^+$, are produced in a 10 Hz laser vaporization source³⁹ coupled to a dual reflectron high resolution time-of-flight mass spectrometer.⁴⁰ In particular, Co and Cr metal targets are ablated by two independent pulsed Nd:YAG lasers at 532 nm. After vaporization, helium gas containing 1% of O_2 is introduced into the source chamber through a pulsed valve to initiate cluster formation. The cluster temperature is estimated to equal the temperature of the cluster source (i.e., 300 K). The validity of this assumption was confirmed in earlier work where argon absorption was used to probe the source temperature.^{41,42} The central part of the cluster beam is selected by a skimmer before entering the extraction chamber, where cationic clusters are accelerated orthogonally into the reflectron time-of-flight mass spectrometer ($m/\Delta m \sim 4000$). The clusters of interest are mass-selected by a wire-type mass gate,^{31,43} installed at the temporal focal point of the first reflectron. Right after the mass gate, the mass-selected clusters are exposed to the third harmonic of a Q-switched Nd:YAG laser (Spectra Physics GCR 150). The laser is slightly defocused to a beam spot of 15 mm diameter and fluences in the range of 10–80 mJ/cm² are used for photodissociation. Based on geometric arguments, the overlap of the laser beam with the ion packet is estimated to be 75%. The photofragments and the remaining parent clusters are mass separated in the second reflectron before being recorded by a microchannel plate detector.

For none of the investigated metal oxide clusters photofragments were obtained at laser fluences lower than 20 mJ/cm². Experiments done by Duncan and co-workers also have shown that a minimal laser fluence is required for photodissociation of transition metal oxide clusters.^{35–38} This likely implies that more than one photon is required to trigger fragmentation. On the other hand not more than two subsequent evaporation events were observed, even with high fluences applied, which indicates that maximally a few photons are absorbed. The fragmentation takes place on the time scale of several microseconds, as confirmed by the observation of dissociation in the second reflectron. This implies that the photofragmentation process occurs via a statistical mechanism,³² which takes place after the electronic energy is converted into ground-state thermal energy.⁴⁴

DFT calculations are performed using the hybrid B3P86 functional^{45,46} in conjunction with the cc-pVTZ and cc-pVTZ-pp (pp stands for a set of pseudopotentials) basis sets as implemented in the GAUSSIAN 09 program.⁴⁷ Structural optimization is done at the B3P86/cc-pVTZ-pp level for Co and Cr and the B3P86/cc-pVTZ level for O. Relative energies of the isomers and dissociation energies are determined on the basis of single-point calculations performed at the optimized structures using the full electron cc-pVTZ basis set.

The B3P86/pVTZ level was selected for the calculation of dissociation energies. The choice of this level resulted from benchmark calculations on dimers, which are presented in the supplementary material.⁴⁸ These benchmark calculations also showed that the DFT approach might be less accurate for describing the metal-metal bonds, but is reliable for metal-oxygen bonds. Since most of the clusters studied in this work only have metal-oxygen bonds (especially those with $n \leq 3$, see further), we are confident that the used computational approach is suitable to predict the relative cluster stability.

III. RESULTS AND DISCUSSIONS

The results and discussion section is divided in four parts. In Subsection III A, the experimental photofragmentation channels of Co_nO_m^+ and $\text{Co}_{n-1}\text{CrO}_m^+$ ($m = 2–6$ for $n = 2, 3$ and $m = 3–8$ for $n = 4$) are analyzed. The influence of the substitution of a Co by a Cr atom on the preferred evaporation channel is highlighted. In Subsection III B, relative stability and indirect structural information as suggested by the photofragmentation data is discussed. In Subsection III C, the calculated structures Co_nO_m^+ and $\text{Co}_{n-1}\text{CrO}_m^+$ ($m = 1–4$ for $n = 2, 3$ and $m = 4$ for $n = 4$) are presented. Finally, in Subsection III D, computed dissociation energies are discussed in terms of the experimentally observed fragmentation channels.

A. Photofragmentation channels

Figure 1 shows selected photofragmentation spectra of pure cobalt oxide and chromium doped cobalt oxide clusters. An overview of the identified dissociation channels of Co_nO_m^+ and $\text{Co}_{n-1}\text{CrO}_m^+$ ($m = 2–6$ for $n = 2, 3$ and $m = 3–8$ for $n = 4$) is given in Table I. We could not mass-select and photofragment $\text{Co}_3\text{CrO}_6^+$ because of its low intensity. For all studied Co_nO_m^+ and $\text{Co}_{n-1}\text{CrO}_m^+$ clusters, the elimination of either an oxygen atom or an oxygen molecule is found to be the preferred dissociation channel. There is no evidence for evaporation of metal atoms, with the exception of Co_3O_2^+ for which the loss of a Co atom is observed as a parallel dissociation channel. Since the detector is unable to record neutral fragments, we can in principle not differentiate between the evaporation of an O_2 molecule or the consecutive evaporation of O atoms, in which case the fragment is denoted as $[\text{O}_2]$. A similar reasoning is followed for $[\text{O}_4]$. In certain cases, laser fluence dependent measurements confirmed the direct evaporation of a O_2 molecule.

Co_2O_2^+ and CoCrO_2^+ are both found to dissociate via the loss of an oxygen atom. Co_2O_3^+ dissociates into Co_2O^+ and a small amount of Co_2O_2^+ . At low laser fluence only the Co_2O^+

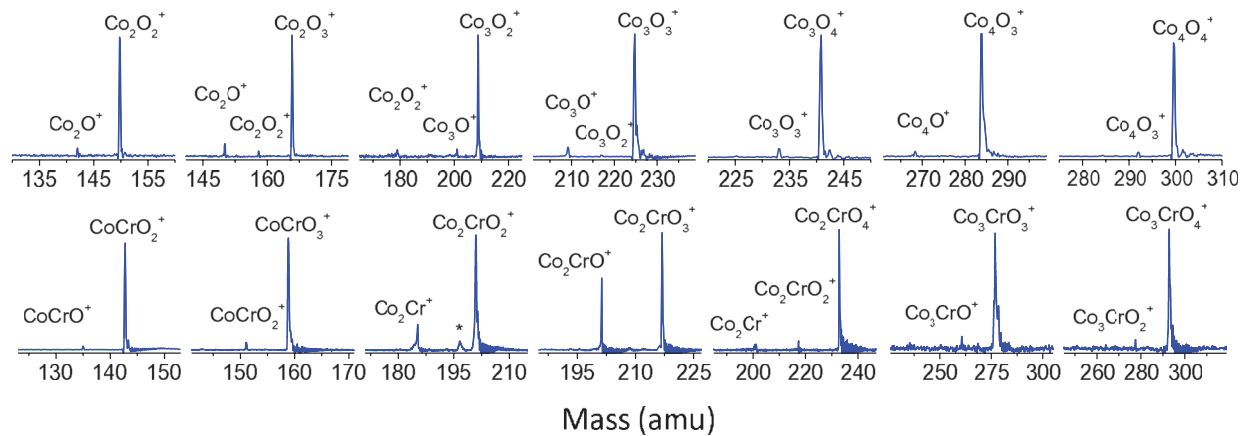


FIG. 1. Mass-selected photofragmentation spectra of $\text{Co}_n \text{O}_m^+$ and $\text{Co}_{n-1} \text{CrO}_m^+$ ($m = 2, 3$ for $n = 2$, $m = 2-4$ for $n = 3$, and $m = 3, 4$ for $n = 4$) with 75 mJ/cm^2 of 355 nm laser light. The peaks with highest intensity correspond to the remaining parent ions. The peak marked with the asterisk corresponds to transmitted $\text{Cr}_2 \text{O}_6^+$ due to the limited resolution of the mass selector.

fragment is observed, which indicates the direct loss of an O_2 molecule rather than sequential evaporation of two O atoms. The alloy cluster CoCrO_3^+ , on the other hand, preferentially dissociates via the loss of a single oxygen atom. The oxygen-rich clusters, $\text{Co}_2 \text{O}_{4-6}^+$ and CoCrO_{4-6}^+ , are found to dissociate via loss of $[\text{O}_2]$.

Evaporation of $[\text{O}_2]$ is the only recorded dissociation channel of the oxygen rich $\text{Co}_3 \text{O}_{5,6}^+$ and the alloy $\text{Co}_2 \text{CrO}_{2-6}^+$ clusters. The dissociation behavior of the oxygen poorer $\text{Co}_3 \text{O}_{2-4}^+$ clusters is different. $\text{Co}_3 \text{O}_2^+$ dissociates via two parallel channels: O and Co atom evaporation, with similar intensities. $\text{Co}_3 \text{O}_3^+$ also decays via two parallel channels, with the loss of O_2 as preferred channel over atomic O evaporation. $\text{Co}_3 \text{O}_4^+$ fragments solely by eliminating oxygen atoms.

Photodissociation spectra of the clusters with four metal atoms show a similar behavior as the smaller sizes. All studied doped clusters, $\text{Co}_3 \text{CrO}_m^+$ with $m = 3-8$, fragment via the loss of $[\text{O}_2]$. The pure cobalt oxide species behave differently. $\text{Co}_4 \text{O}_3^+$ loses $[\text{O}_2]$, while $\text{Co}_4 \text{O}_4^+$ evaporates an O atom.

$\text{Co}_4 \text{O}_5^+$ has two parallel evaporation channels, corresponding to the loss of O and O_2 , with $\text{Co}_4 \text{O}_3^+$ being the most intense fragment.

In summary, the photodissociation spectra show that the substitution of a single Co by a Cr atom in $\text{Co}_n \text{O}_m^+$ has an influence on the preferred evaporation channel. Whereas all $\text{Co}_{n-1} \text{CrO}_m^+$ clusters (except $\text{CoCrO}_{2,3}^+$) prefer to decay by elimination of $[\text{O}_2]$ units, several pure $\text{Co}_n \text{O}_m^+$ clusters evaporate atomic oxygen.

The present results for the pure $\text{Co}_n \text{O}_m^+$ can be compared with previous experimental dissociation studies. This comparison is summarized in Table II. Collision-induced dissociation of oxygen-equivalent $\text{Co}_n \text{O}_n^+$ and oxygen-deficient $\text{Co}_n \text{O}_{n-1}^+$ ($n = 2-5$) clusters was studied by Freas and coworkers.²³ Johnson *et al.* reported the influence of stoichiometry and charge state on the structure of $\text{Co}_n \text{O}_m^{0,+}$ ($n = 1, 2$ and $m = 2-6$).²⁷ Recently, photodissociation investigations of $\text{Co}_n \text{O}_m^+$ ($n = 4-9$, $m = 4-17$) clusters by Dibble *et al.* demonstrated the high stability of $\text{Co}_4 \text{O}_4^+$.³⁵ It was also

TABLE I. Evaporation channels and fragment ions resulting from photodissociation of $\text{Co}_n \text{O}_m^+$ and $\text{Co}_{n-1} \text{CrO}_m^+$. The most intense fragment is listed first. A slash is used to separate parallel fragmentation channels.

| Parent cluster | Fragment ion | Evaporation channel | Parent cluster | Fragment ion | Evaporation channel |
|----------------------------|---|------------------------------|------------------------------|---|------------------------------|
| $\text{Co}_2 \text{O}_2^+$ | $\text{Co}_2 \text{O}^+$ | O | CoCrO_2^+ | CoCrO^+ | O |
| $\text{Co}_2 \text{O}_3^+$ | $\text{Co}_2 \text{O}^+ / \text{Co}_2 \text{O}_2^+$ | O_2, O | CoCrO_3^+ | CoCrO_2^+ | O |
| $\text{Co}_2 \text{O}_4^+$ | $\text{Co}_2 \text{O}_2^+$ | $[\text{O}_2]$ | CoCrO_4^+ | CoCrO_2^+ | $[\text{O}_2]$ |
| $\text{Co}_2 \text{O}_5^+$ | $\text{Co}_2 \text{O}_3^+$ | $[\text{O}_2]$ | CoCrO_5^+ | CoCrO_3^+ | $[\text{O}_2]$ |
| $\text{Co}_2 \text{O}_6^+$ | $\text{Co}_2 \text{O}_2^+$ | $[\text{O}_4]$ | CoCrO_6^+ | CoCrO_4^+ | $[\text{O}_2]$ |
| $\text{Co}_3 \text{O}_2^+$ | $\text{Co}_3 \text{O}^+ / \text{Co}_2 \text{O}_2^+$ | O/Co | $\text{Co}_2 \text{CrO}_2^+$ | $\text{Co}_2 \text{Cr}^+$ | $[\text{O}_2]$ |
| $\text{Co}_3 \text{O}_3^+$ | $\text{Co}_3 \text{O}^+ / \text{Co}_3 \text{O}_2^+$ | O_2 / O | $\text{Co}_2 \text{CrO}_3^+$ | $\text{Co}_2 \text{CrO}^+$ | $[\text{O}_2]$ |
| $\text{Co}_3 \text{O}_4^+$ | $\text{Co}_3 \text{O}_3^+$ | O | $\text{Co}_2 \text{CrO}_4^+$ | $\text{Co}_2 \text{CrO}_2^+, \text{Co}_2 \text{Cr}^+$ | $[\text{O}_2], [\text{O}_4]$ |
| $\text{Co}_3 \text{O}_5^+$ | $\text{Co}_3 \text{O}_3^+$ | $[\text{O}_2]$ | $\text{Co}_2 \text{CrO}_5^+$ | $\text{Co}_2 \text{CrO}_3^+$ | $[\text{O}_2]$ |
| $\text{Co}_3 \text{O}_6^+$ | $\text{Co}_3 \text{O}_4^+$ | $[\text{O}_2]$ | $\text{Co}_2 \text{CrO}_6^+$ | $\text{Co}_2 \text{CrO}_4^+$ | $[\text{O}_2]$ |
| $\text{Co}_4 \text{O}_3^+$ | $\text{Co}_4 \text{O}^+$ | $[\text{O}_2]$ | $\text{Co}_3 \text{CrO}_3^+$ | $\text{Co}_3 \text{CrO}^+$ | $[\text{O}_2]$ |
| $\text{Co}_4 \text{O}_4^+$ | $\text{Co}_4 \text{O}_3^+$ | O | $\text{Co}_3 \text{CrO}_4^+$ | $\text{Co}_3 \text{CrO}_2^+$ | $[\text{O}_2]$ |
| $\text{Co}_4 \text{O}_5^+$ | $\text{Co}_4 \text{O}_3^+ / \text{Co}_4 \text{O}_4^+$ | O_2 / O | $\text{Co}_3 \text{CrO}_5^+$ | $\text{Co}_3 \text{CrO}_3^+$ | $[\text{O}_2]$ |
| $\text{Co}_4 \text{O}_6^+$ | $\text{Co}_4 \text{O}_4^+$ | $[\text{O}_2]$ | ... | ... | ... |
| $\text{Co}_4 \text{O}_7^+$ | $\text{Co}_4 \text{O}_5^+, \text{Co}_4 \text{O}_3^+$ | $[\text{O}_2], [\text{O}_4]$ | $\text{Co}_3 \text{CrO}_7^+$ | $\text{Co}_3 \text{CrO}_5^+$ | $[\text{O}_2]$ |
| $\text{Co}_4 \text{O}_8^+$ | $\text{Co}_4 \text{O}_4^+$ | $[\text{O}_4]$ | $\text{Co}_3 \text{CrO}_8^+$ | $\text{Co}_3 \text{CrO}_6^+$ | $[\text{O}_2]$ |

TABLE II. Comparison of the Co_nO_m^+ dissociation channels observed in the present study with results available in literature. The most intense channel, if applicable, is listed in bold.

| Parent | This work | Others |
|---------------------------|-------------------|--|
| Co_2O_2^+ | O | O, O_2 , CoO, CoO_2^a O_2, O_4^b |
| Co_2O_4^+ | $[\text{O}_2]$ | O_2, O_4^b |
| Co_2O_6^+ | $[\text{O}_2]$ | $\text{O}_2, \text{O}_4, \text{O}_5, \text{CoO}_2, \text{CoO}_4^b$ |
| Co_3O_2^+ | O, Co | Co, CoO , Co_2O_2^a |
| Co_3O_3^+ | O, $[\text{O}_2]$ | O, O_2 , CoO, CoO_2 , Co_2O_2 , Co_2O_3^a |
| Co_4O_3^+ | $[\text{O}_2]$ | Co, CoO, Co_2O_2 , Co_3O_3^a |
| Co_4O_4^+ | O | CoO , CoO_2 , Co_2O_2 , Co_2O_3 , Co_3O_4^a Co, CoO, CoO_2^c |
| Co_4O_5^+ | O, O_2 | O, O_2 , CoO_2^c |
| Co_4O_6^+ | $[\text{O}_2]$ | O_2 , CoO_2^c |
| Co_4O_7^+ | $[\text{O}_2]$ | $\text{O}_2, \text{O}_3, \text{O}_4$, CoO_4^c |

^aReference 23.

^bReference 27.

^cReference 35.

suggested that Co_nO_m^+ dissociates preferentially via the loss of O_2 and that fragment ions with a 1:1 stoichiometry are favored.³⁵ Under the experimental conditions of these earlier studies, nevertheless, multiple fragment ions are found in most cases, causing ambiguity to identify sequential/parallel dissociation channels. In addition, it is also difficult to determine whether the losses of observed larger neutral fragments result from a single dissociation event or multiple consecutive ones. Possibly, in those cited studies higher laser fluences were used or the clusters initially had a higher internal energy. In the present study, the preferred dissociation channels of Co_nO_m^+ and $\text{Co}_{n-1}\text{CrO}_m^+$ clusters can clearly be distinguished and there is no evidence for the occurrence of multiple subsequent evaporation events.

B. Relative stability and structural information from the photofragmentation data

The mass spectrometric results and the photofragmentation channels provide direct information on the relative stability and indirect qualitative information on the structure of the clusters.

The intensities of clusters, as produced in the source, are not only determined by relative stability but also by growth conditions (e.g., temperature of the cluster source, partial pressure of the inert gasses used for the condensation, etc.) and size-dependent ionization energies. In contrast, in the present experiments, where clusters are first mass-selected and then exposed to laser light, the fragmentation process tends to terminate at fragment ions with an enhanced stability. High internal energy of the clusters after photoabsorption allows the clusters to explore (on average) the most stable structural configuration.

The data listed in Table I show that Co_2O_2^+ , Co_4O_3^+ , and Co_4O_4^+ are produced frequently as fragment of larger clusters, implying that they are relatively stable. Specifically, Co_2O_2^+ is a fragment of Co_2O_3^+ , Co_2O_4^+ , Co_2O_6^+ , and Co_3O_2^+ . Co_2O_2^+ may even be more stable than Co_2O_2^+ , since it is the most intense fragment of Co_2O_3^+ (see Fig. 1). Co_4O_3^+ is a daugh-

ter ion of Co_4O_4^+ , Co_4O_5^+ , and Co_4O_7^+ , while dissociation of Co_4O_5^+ , Co_4O_6^+ , and Co_4O_8^+ terminates at Co_4O_4^+ . The enhanced stability of Co_4O_4^+ was also observed in Ref. 35.

Qualitative stability information can be obtained from the relative intensities of fragment to parent signals. It is expected that the more stable clusters tend to remain more intense after fragmentation.^{31,33} The proposed enhanced stability of Co_2O_2^+ , Co_4O_3^+ , and Co_4O_4^+ is consistent with this argument. It should also be mentioned that a high fluence ($>50 \text{ mJ/cm}^2$) was needed to fragment CoCrO_2^+ while the other clusters could be fragmented at a fluence threshold of about 20 mJ/cm^2 . It implies that CoCrO_2^+ is a relatively more stable cluster. Alternatively, $\text{Co}_2\text{CrO}_2^+$ and $\text{Co}_2\text{CrO}_3^+$ could easily be fragmented, suggesting that they might be relatively less stable than their pure counterparts, Co_3O_2^+ and Co_3O_3^+ . It should be noted that these conclusions are only valid if the photoabsorption cross-sections do not strongly vary in the investigated size range, for which there is no independent evidence.

The preferred dissociation channels can also provide hints about the structures of the clusters, e.g., whether oxygen prefers integrating into the metallic framework or being weakly adsorbed to the surface.^{35,38} Possibly the atomic oxygen evaporation channel implies that Co_nO_m^+ with $m \leq n + 1$ for $n = 2, 3$ and $m \leq n$ for $n = 4$ have structures in which oxygen atoms bridge the metal atoms. The $[\text{O}_2]$ loss channel of the oxygen-rich species might imply that they have weakly attached O_2 units. The preferred loss of $[\text{O}_2]$ for most Cr-doped species suggests that doping may modify the metal-oxygen framework. Since CoCrO_3^+ favors the loss of an O atom to form the stable CoCrO_2^+ , one might postulate that the third O atom in CoCrO_3^+ is not bridging the Co and Cr atoms. Structural argumentation based on photodissociation experiments, however, has to be treated with care. The high photoexcitation energy may cause structural permutation before fragmentation. During this process the clusters explore all possibilities of getting the energetically most favorable dissociation channel. In this context, DFT computations provide additional information for structural determination.

C. Calculated structures of the Co_nO_m^+ and $\text{Co}_{n-1}\text{CrO}_m^+$

The most stable isomers of Co_nO_m^+ and $\text{Co}_{n-1}\text{CrO}_m^+$ ($m = 1-4$ for $n = 2, 3$ and $m = 3, 4$ for $n = 4$), as obtained at the computational level described in Sec. II, and the relative energies of those isomers with respect to the obtained lowest energy structures are given in Fig. 2. Descriptions of the structures are available in the supplementary material.⁴⁸ We found that for both pure and doped species, oxygen atoms prefer to bind atomically to the metal atoms until the number of oxygen-metal bonds is maximized. Additional oxygen atoms are adsorbed to the metal-oxygen framework. The minimum-energy structures (MES) of clusters containing more than one oxygen atom often are ring-based geometries, except for Co_2O_2^+ , Co_2O_3^+ , $\text{Co}_2\text{CrO}_2^+$, and $\text{Co}_3\text{CrO}_4^+$. The linear MES obtained for Co_2O_2^+ is unexpected in comparison with previous predictions for $\text{Co}_2\text{O}_2^{0,+}$, where ring structures were found to be most stable.^{22,27} Linear MES structures are also found

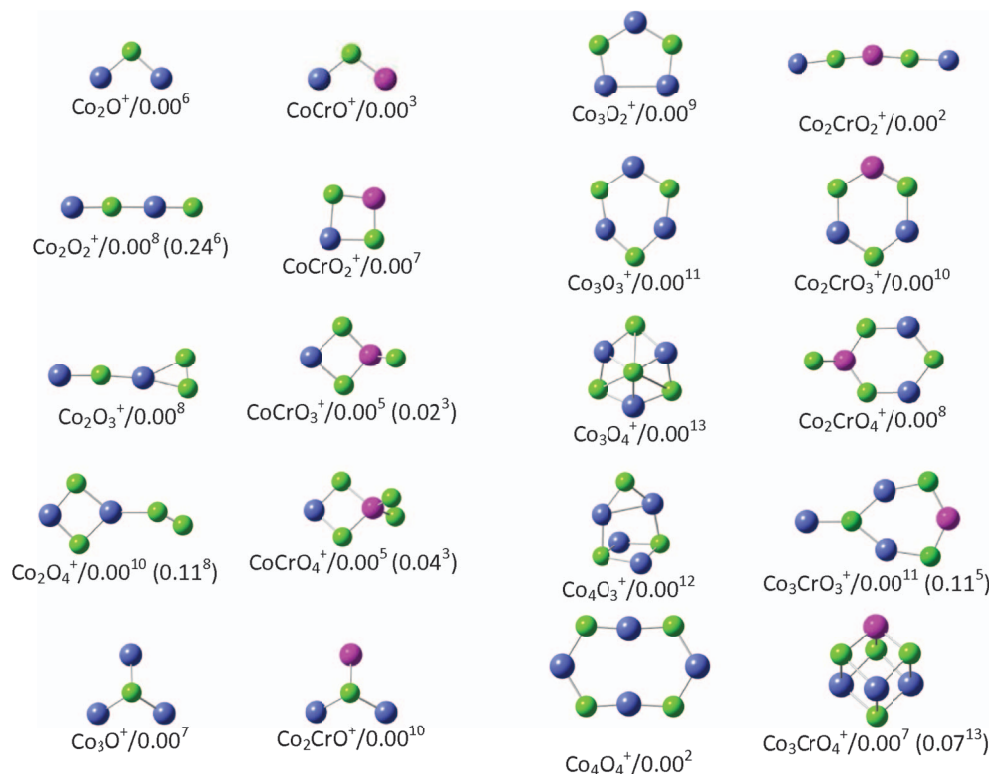


FIG. 2. Optimized ground-state structures, relative energies (in eV), and spin multiplicities (superscript) of Co_nO_m^+ and $\text{Co}_{n-1}\text{CrO}_m^+$ ($m = 1-4$ for $n = 2, 3$ and $m = 3, 4$ for $n = 4$).

for Co_2O_3^+ and $\text{Co}_2\text{CrO}_2^+$. The replacement of a Co by a Cr atom in Co_4O_4^+ induces a complete geometric restructuring, with the most stable form of $\text{Co}_3\text{CrO}_4^+$ being a cube.

In good agreement with the suggestions based on the experimental dissociation pathways, Co_nO_m^+ with $m \leq n + 1$ for $n = 2, 3$ and $n, m = 4$ have structures with metal-oxygen bonds and adsorbed oxygen atoms. The experimentally observed $[\text{O}_2]$ loss of Co_2O_4^+ is also supported by the predicted ring-based ground-state structure with a weakly bound O_2 unit. The structural difference between an almost linear Co_2O_3^+ and a ring structure with an attached O atom for CoCrO_3^+ is reflected in the preferred dissociation channels (evaporation of O_2 molecule and an O atom, respectively). Similarly, different experimentally observed dissociation behavior for pairs of pure Co_nO_m^+ clusters and Cr doped clusters, such as, Co_3O_2^+ and $\text{Co}_2\text{CrO}_2^+$, Co_3O_4^+ and $\text{Co}_2\text{CrO}_4^+$, and Co_4O_4^+ and $\text{Co}_3\text{CrO}_4^+$, may be explained on the basis of their different geometrical structures.

D. Dissociation energies

The calculated dissociation energy required to remove atomic oxygen [DE(O)], molecular oxygen [DE(O_2)], and a Co or a Cr atom, [DE(Co)] and [DE(Cr)], from the cobalt oxide clusters and their Cr-doped counterparts are listed in Table III. Those energy differences between the parent cluster and the fragments are calculated assuming lowest energy structures (and spin states) for the mother cluster and the fragments. The expected error margin of the current DFT functional on thermodynamic parameters is about ± 0.3 eV.

Dissociation channels involving species with metal-metal bonds are marked with †, and are likely less accurate given the current description of metal-metal bonds at the applied DFT level (cf. the discussion on the benchmark data for dimers in the supplementary material⁴⁸). It is expected from detailed balance theory that the evaporative rate constant $k_n(E)$ depends strongly on the dissociation energy.³⁰⁻³² The preferred evaporation channel thus corresponds to the channel with the lowest dissociation energy.

TABLE III. Calculated dissociation energies (in eV) to remove atomic oxygen, DE(O), molecular oxygen, DE(O_2), and a Co or Cr atom, DE(Co), and DE(Cr). The experimentally preferred fragments are listed for comparison.

| Parents | DE(O) | DE(O_2) | DE(Co) | DE(Cr) | Preferred fragments |
|-----------------------------|-------------------|--------------------|-------------------|--------|---------------------|
| Co_2O_2^+ | 3.31 | 2.95 ^a | 4.29 | ... | O |
| Co_2O_3^+ | 3.49 | 1.27 | 4.72 | ... | O_2 |
| Co_2O_4^+ | 3.32 | 1.28 | 4.74 | ... | $[\text{O}_2]$ |
| CoCrO_2^+ | 4.88 | 5.58 ^a | 5.15 | 6.28 | O |
| CoCrO_3^+ | 4.34 | 3.69 | 5.88 | 7.56 | O |
| CoCrO_4^+ | 2.98 | 1.79 | 5.99 | 7.24 | $[\text{O}_2]$ |
| Co_3O_2^+ | 4.73 ^a | 4.23 ^a | 3.93 ^a | ... | O/Co |
| Co_3O_3^+ | 5.48 | 4.68 | 5.92 | ... | O_2 |
| Co_3O_4^+ | 2.33 | 2.28 ^a | 4.93 | ... | O |
| $\text{Co}_2\text{CrO}_2^+$ | 5.57 ^a | 6.38 ^a | 3.04 | 5.03 | $[\text{O}_2]$ |
| $\text{Co}_2\text{CrO}_3^+$ | 5.40 | 5.44 | 4.10 | 6.95 | $[\text{O}_2]$ |
| $\text{Co}_2\text{CrO}_4^+$ | 4.37 | 4.24 | 5.49 | 7.99 | $[\text{O}_2]$ |
| Co_4O_3^+ | 5.73 ^a | 5.49 ^a | 3.31 ^a | ... | $[\text{O}_2]$ |
| Co_4O_4^+ | 4.86 ^a | 5.06 ^a | 5.85 | ... | O |
| $\text{Co}_3\text{CrO}_3^+$ | 5.83 ^a | 6.02 ^a | 3.04 | 4.06 | $[\text{O}_2]$ |
| $\text{Co}_3\text{CrO}_4^+$ | 5.57 | 5.87 ^a | 4.24 | 7.31 | $[\text{O}_2]$ |

^aDissociation channels involving clusters with metal-metal bonds.

The values in Table III indicate that the Cr doped species are relatively more stable than the pure cobalt oxide clusters. In particular, Cr doping significantly enhances the stability of Co_3O_4^+ . At least 4.24 eV is needed to fragment $\text{Co}_2\text{CrO}_4^+$, while only 2.28 eV is needed for dissociation of Co_3O_4^+ . This enhanced stability of $\text{Co}_{n-1}\text{CrO}_m^+$ compared to Co_nO_m^+ could be explained by the larger binding energy of CrO (4.36 ± 0.3 eV) than that of CoO (3.98 ± 0.14 eV).⁴⁹

For $n = 2$ species, the calculations indicate that Co_2O_3^+ , Co_2O_4^+ , and CoCrO_4^+ prefer to dissociate by loss of an oxygen molecule. This implies that the experimental observations indeed correspond to the loss of O_2 , rather than the consecutive evaporation of two O atoms. Also the experimentally observed atomic O evaporation from CoCrO_2^+ is confirmed by the calculations. For Co_2O_2^+ and CoCrO_3^+ , the calculations indicate that evaporation of molecular oxygen is the most facile dissociation channel, while the experiments show atomic oxygen evaporation. The relative energy differences between $\text{DE}(\text{O})$ and $\text{DE}(\text{O}_2)$ for these clusters is, however, comparable to the computational error margin.

For the $n = 3$ species, the calculations predict that Co_3O_2^+ , $\text{Co}_2\text{CrO}_2^+$, and $\text{Co}_2\text{CrO}_3^+$ prefer dissociating via the loss of a Co atom, while other species favor evaporation of either an oxygen atom or an oxygen molecule. The evaporation of a Co atom for Co_3O_2^+ is in line with the experimental observations, where the loss of a Co and an O atom are observed as parallel channels. Also the observed O_2 loss channels for Co_3O_3^+ and $\text{Co}_2\text{CrO}_4^+$ are confirmed by the calculations. The calculated energy difference between $\text{DE}(\text{O})$ and $\text{DE}(\text{O}_2)$ for Co_3O_4^+ is much smaller than the error margin, which implies that the calculations support the experiments. The calculated DEs of $\text{Co}_2\text{CrO}_2^+$ and $\text{Co}_2\text{CrO}_3^+$ show that the most facile channel is the evaporation of a Co atom. It should also be remarked that a high daughter/parent intensity ratio is observed for $\text{Co}_2\text{CrO}_3^+$ (see Fig. 1), while this cluster is predicted to have a relatively high DE. This likely implies that the photoabsorption efficiency of this cluster is high at 355 nm.

For the $n = 4$ species, the calculations show that oxygen atom evaporation is the energetically preferred channel for Co_4O_4^+ , which is in good agreement with the experimental observation. For Co_4O_3^+ , $\text{Co}_3\text{CrO}_3^+$, and $\text{Co}_3\text{CrO}_4^+$, the calculations indicate that the evaporation of a Co atom is the preferred dissociation path, whereas the experiments show the loss of $[\text{O}_2]$ as most facile channel. These differences could be related to the inherent shortcoming in the energetic treatment of metal-metal bonds using DFT methods, which is difficult to overcome, in particular for larger sized species. Alternatively, the differences could be due to kinetic-controlled processes, where an activation energy is needed to initiate dissociation. The presence of a possible energy barrier has not been taken into account in the present calculations. In this context, the overall agreement between calculated dissociation energies and experimental observations, especially for $n = 2$ and $n = 3$, is satisfactory.

IV. CONCLUSIONS

We have investigated the stability of pure cobalt oxide and chromium doped cobalt oxide clusters Co_nO_m^+ and

$\text{Co}_{n-1}\text{CrO}_m^+$ ($n = 2, 3$; $m = 2-6$ and $n = 4$; $m = 3-8$), by means of photodissociation experiments in combination with DFT calculations. Photofragmentation spectra prove that pure cobalt oxide clusters with a high oxygen content ($m \geq n + 1$ for $n = 2, 4$ and $m \geq n + 2$ for $n = 3$) favor splitting off molecular oxygen. Clusters with a lower oxygen content prefer to evaporate atomic oxygen. Substitution of a Co by a Cr atom alters the dissociation behavior. For all studied chromium doped species, except for CoCrO_2^+ and CoCrO_3^+ , $[\text{O}_2]$ unit evaporation is experimentally found to be the most facile dissociation channel.

DFT calculations demonstrate that most of the investigated Co_nO_m^+ and $\text{Co}_{n-1}\text{CrO}_m^+$ ($m = 1-4$ for $n = 2, 3$ and $m = 3, 4$ for $n = 4$) clusters have structures in which the number of metal-oxygen bonds is maximized. The dopant atom has the strongest influence on the geometric structure for CoCrO_3^+ , $\text{Co}_2\text{CrO}_2^+$, $\text{Co}_2\text{CrO}_4^+$, and $\text{Co}_3\text{CrO}_4^+$, suggesting a different growth mechanism compared with the undoped cobalt oxide clusters. These structural changes are supported by corresponding changes in their measured dissociation behavior. The calculated most facile dissociation channels generally are in good agreement with the experimental observations. Detailed comparison between experimental dissociation behavior and computational data show that Co_2O_2^+ , CoCrO_2^+ , Co_4O_3^+ , and Co_4O_4^+ are particularly stable. The calculated dissociation energies suggest an enhanced stability of the Cr doped clusters over their pure counterparts. The enhanced stability by Cr doping is not directly observed in the fragmentation spectra where daughter/parent intensity ratios are higher for the doped species (in particular for $\text{Co}_2\text{CrO}_2^+$ and $\text{Co}_2\text{CrO}_3^+$). Those findings are not conflicting if the photoabsorption efficiency of these clusters at 355 nm is enhanced by Cr doping.

ACKNOWLEDGMENTS

This work is supported by the Research Foundation - Flanders (FWO), by the KU Leuven Research Council (BOF, GOA, and IDO programs), and by the COST action MP0903 - Nanoalloy.

¹V. E. Henrich and P. A. Cox, *The Surface Science of Metal Oxides* (Cambridge University Press, Cambridge, 1994).

²G. A. Samorjai, *Introduction to Surface Chemistry and Catalysis* (Wiley Interscience, New York, 1994).

³P. A. Cox, *Transition Metal Oxides* (Clarendon, Oxford, 1992).

⁴C. N. Rao and B. Raveau, *Transition Metal Oxides* (Wiley, New York, 1998).

⁵W. Eerenstein, N. D. Mathur, and J. F. Scott, *Nature (London)* **442**, 759 (2006).

⁶G. R. Patzke, Y. Zhou, R. Kontic, and F. Conrad, *Angew. Chem.: Int. Ed.* **50**, 826 (2011).

⁷J. A. Alonso, *Chem. Rev.* **100**, 637 (2000).

⁸J. Garcia-Barriocanal, A. Rivera-Calzada, M. Varela, Z. Sefrioui, M. R. Diaz-Guillen, K. J. Moreno, J. A. Diaz-Guillen, E. Iborra, A. F. Fuentes, S. J. Pennycook, C. Leon, and J. Santarnaria, *ChemPhysChem* **10**, 1003 (2009).

⁹K. R. Asmis, *Phys. Chem. Chem. Phys.* **14**, 9270 (2012).

¹⁰H. J. Zhai, X. Huang, T. Waters, X. B. Wang, R. A. J. O'Hair, A. G. Wedd, and L. S. Wang, *J. Phys. Chem. A* **109**, 10512 (2005).

¹¹E. Janssens, G. Santambrogio, M. Brummer, L. Wöste, P. Lievens, J. Sauer, G. Meijer, and K. R. Asmis, *Phys. Rev. Lett.* **96**, 233401 (2006).

- ¹²N. J. Mayhall, D. W. Rothgeb, E. Hossain, K. Raghavachari, and C. C. Jarrold, *J. Chem. Phys.* **130**, 124313 (2009).
- ¹³J. E. Mann, D. W. Rothgeb, S. E. Waller, and C. C. Jarrold, *J. Phys. Chem. A* **114**, 11312 (2010).
- ¹⁴L. Jiang, T. Wende, P. Claes, S. Bhattacharyya, M. Sierka, G. Meijer, P. Lievens, J. Sauer, and K. R. Asmis, *J. Phys. Chem. A* **115**, 11187 (2011).
- ¹⁵M. W. Kanan and D. G. Nocera, *Science* **321**, 1072 (2008).
- ¹⁶D. A. Lutterman, Y. Surendranath, and D. G. Nocera, *J. Am. Chem. Soc.* **131**, 3838 (2009).
- ¹⁷M. D. Symes, Y. Surendranath, D. A. Lutterman, and D. G. Nocera, *J. Am. Chem. Soc.* **133**, 5174 (2011).
- ¹⁸C. J. Jia, M. Schwickardi, C. Weidenthaler, W. Schmidt, S. Korhonen, B. M. Weckhuysen, and F. Schuth, *J. Am. Chem. Soc.* **133**, 11279 (2011).
- ¹⁹V. Skumryev, S. Stoyanov, Y. Zhang, G. Hadjipanayls, D. Givord, and J. Nogues, *Nature (London)* **423**, 850 (2003).
- ²⁰P. Poizot, S. Laruelle, S. Grugeon, L. Dupont, and J. M. Tarascon, *Nature (London)* **407**, 496 (2000).
- ²¹M. J. Benitez, O. Petravic, H. Tuysuz, F. Schuth, and H. Zabel, *Europhys. Lett.* **88**, 27004 (2009).
- ²²S. Yin, W. Xue, X. L. Ding, W. G. Wang, S. G. He, and M. F. Ge, *Int. J. Mass Spectrom.* **281**, 72 (2009).
- ²³R. B. Freas, B. I. Dunlap, B. A. Waite, and J. E. Campana, *J. Chem. Phys.* **86**, 1276 (1987).
- ²⁴G. V. Chertihin, A. Citra, L. Andrews, and C. W. Bauschlicher, Jr., *J. Phys. Chem. A* **101**, 8793 (1997).
- ²⁵A. Pramann, K. Koyasu, A. Nakajima, and K. Kaya, *J. Phys. Chem. A* **106**, 4891 (2002).
- ²⁶F. Liu, F. X. Li, and P. B. Armentrout, *J. Chem. Phys.* **123**, 064304 (2005).
- ²⁷G. E. Johnson, J. U. Reveles, N. M. Reilly, E. C. Tyo, S. N. Khanna, and A. W. Castleman, Jr., *J. Phys. Chem. A* **112**, 11330 (2008).
- ²⁸Y. Yamasaki, S. Miyasaka, Y. Kaneko, J. P. He, T. Arima, and Y. Tokura, *Phys. Rev. Lett.* **96**, 207204 (2006).
- ²⁹Y. J. Choi, J. Okamoto, D. J. Huang, K. S. Chao, H. J. Lin, C. T. Chen, M. van Veenendaal, T. A. Kaplan, and S. W. Cheong, *Phys. Rev. Lett.* **102**, 067601 (2009).
- ³⁰L. Schweikhard, K. Hansen, A. Herlert, M. D. Herranz Lablanca, and M. Vogel, *Eur. Phys. J. D* **36**, 179 (2005).
- ³¹N. Veldeman, E. Janssens, K. Hansen, J. De Haeck, R. E. Silverans, and P. Lievens, *Faraday Discuss.* **138**, 147 (2007).
- ³²S. Bhattacharyya, T. T. Nguyen, J. De Haeck, K. Hansen, P. Lievens, and E. Janssens, *Phys. Rev. B* **87**, 054103 (2013).
- ³³N. T. Tung, E. Janssens, S. Bhattacharyya, and P. Lievens, *Eur. Phys. J. D* **67**, 41 (2013).
- ³⁴J. B. Jaeger, T. D. Jaeger, and M. A. Duncan, *J. Phys. Chem. A* **110**, 9310 (2006).
- ³⁵C. J. Dibble, S. T. Akin, S. Ard, C. P. Fowler, and M. A. Duncan, *J. Phys. Chem. A* **116**, 5398 (2012).
- ³⁶K. S. Molek, Z. D. Reed, A. M. Ricks, and M. A. Duncan, *J. Phys. Chem. A* **111**, 8080 (2007).
- ³⁷K. S. Molek, T. D. Jaeger, and M. A. Duncan, *J. Chem. Phys.* **123**, 144313 (2005).
- ³⁸K. S. Molek, C. Anfuso-Cleary, and M. A. Duncan, *J. Phys. Chem. A* **112**, 9238 (2008).
- ³⁹W. Bouwen, P. Thoen, F. Vanhoutte, S. Bouckaert, F. Despa, H. Weidele, R. E. Silverans, and P. Lievens, *Rev. Sci. Instrum.* **71**, 54 (2000).
- ⁴⁰J. De Haeck, "Mass spectrometric developments and a study of lithium doped silicon and germanium clusters," Ph.D. thesis (KU Leuven, 2011).
- ⁴¹E. Janssens, P. Gruene, G. Meijer, L. Wöste, P. Lievens, and A. Fielicke, *Phys. Rev. Lett.* **99**, 063401 (2007).
- ⁴²S. M. Lang, P. Claes, N. T. Cuong, M. T. Nguyen, P. Lievens, and E. Janssens, *J. Chem. Phys.* **135**, 224305 (2011).
- ⁴³P. R. Vlasak, D. J. Beussman, M. R. Davenport, and C. G. Enke, *Rev. Sci. Instrum.* **67**, 68 (1996).
- ⁴⁴A. Terasaki, *J. Phys. Chem. A* **111**, 7671 (2007).
- ⁴⁵A. D. Becke, *J. Chem. Phys.* **98**, 5648 (1993).
- ⁴⁶J. P. Perdew, *Phys. Rev. B* **33**, 8822 (1986).
- ⁴⁷M. J. Frisch, G. W. Trucks, H. B. Schlegel *et al.*, GAUSSIAN 09, Revision B.01, Gaussian, Inc., Wallingford, CT, 2009.
- ⁴⁸See supplementary material at <http://dx.doi.org/10.1063/1.4890500> for benchmark data on dimers used to select the DFT level and for optimized structures of energetically low-lying isomers of the Co_nO_m^+ and $\text{Co}_{n-1}\text{CrO}_m^+$ clusters.
- ⁴⁹Y. R. Luo, *Comprehensive Handbook of Chemical Bond Energies* (CRC Press, Boca Raton, FL, 2007).